Selective Synthesis and Device Applications of Semiconducting Single-Walled Carbon Nanotubes Using Isopropyl Alcohol as Feedstock

Yuchi Che,[†,§] Chuan Wang,[†,§] Jia Liu,[†,§] Bilu Liu,[†] Xue Lin,[†] Jason Parker,[‡] Cara Beasley,[‡] H.-S. Philip Wong,[‡,*] and Chongwu Zhou[†,*]

[†]Department of Electrical Engineering, University of Southern California, Los Angeles, California 90089, United States and [‡]Department of Electrical Engineering, Stanford University, Stanford, California 94305, United States. [§]These authors contributed equally to this work.

ABSTRACT

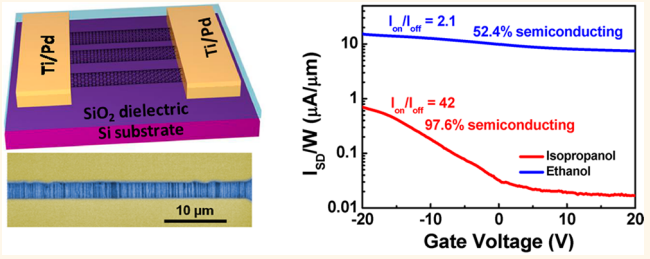

The development of guided chemical vapor deposition (CVD) growth of single-walled carbon nanotubes provides a great platform for wafer-scale integration of aligned nanotubes into circuits and functional electronic systems. However, the coexistence of metallic and semiconducting nanotubes is still a major obstacle for the development of carbon-nanotube-based nanoelectronics. To address this problem, we have developed a method to obtain predominantly semiconducting nanotubes from direct CVD growth. By using isopropyl alcohol (IPA) as the carbon feedstock, a semiconducting nanotube purity of above 90% is achieved, which is unambiguously confirmed by both electrical and micro-Raman measurements. Mass spectrometric study was performed to elucidate the underlying chemical mechanism. Furthermore, high performance thin-film transistors with an on/off ratio above 10^4 and mobility up to 116 $cm^2/(V \cdot s)$ have been achieved using the IPA-synthesized nanotube networks grown on silicon substrate. The method reported in this contribution is easy to operate and the results are highly reproducible. Therefore, such semiconducting predominated single-walled carbon nanotubes could serve as an important building block for future practical and scalable carbon nanotube electronics.

KEYWORDS: carbon nanotube · semiconducting · controlled synthesis · transistor · quartz · silicon substrate

The outstanding potential of using carbon nanotubes for beyond-silicon nanoelectronics stems from the fact that they offer a combination of small size, high mobility, ballistic transport, and small intrinsic capacitance.[1−9] However, one of the major challenges remaining to be solved is how to make the nanotube electronics practical and scalable. To address this issue, the guided chemical vapor deposition (CVD) growth of horizontally aligned single-walled carbon nanotubes on certain crystalline substrates like quartz and sapphire developed by many groups including our own[10−12] is proven to be a great platform for wafer-scale integration of aligned nanotubes into circuits and functional electronic systems.[9,13,14] Owing to significant effort devoted to the synthesis of single-walled carbon nanotubes, high density and good alignment have been achieved in previous studies,[15−17] which provide great advantage on the device performance of nanotube electronics. However, the coexistence of metallic and semiconducting nanotubes still remains a major problem that hampers further development of nanoelectronics based on carbon nanotubes. To solve this problem, selective elimination using electrical breakdown is widely used for device study.[18] However, this technique hurts the conductivity of nanotubes and is hardly scalable to systems containing millions or billions of transistors. Meanwhile, methods of separating metallic nanotubes from semiconducting ones have been studied by using various approaches.[19−22] However, chemical separation treatment induces defects in nanotubes and leads to contamination, which degrades the performance of nanotubes in terms of mobility. Therefore, it is very desirable to achieve controlled growth of semiconducting nanotubes through CVD directly.

Previously, semiconducting enriched nanotubes have been synthesized using techniques such as gas phase[23] and supported catalyst CVD.[24−26] However, those nanotubes typically come as bundles and consequently cannot be easily used for nanoelectronic

* Address correspondence to chongwuz@usc.edu, hspwong@stanford.edu.

Received for review June 20, 2012 and accepted July 31, 2012.

Published online July 31, 2012
10.1021/nn302720n

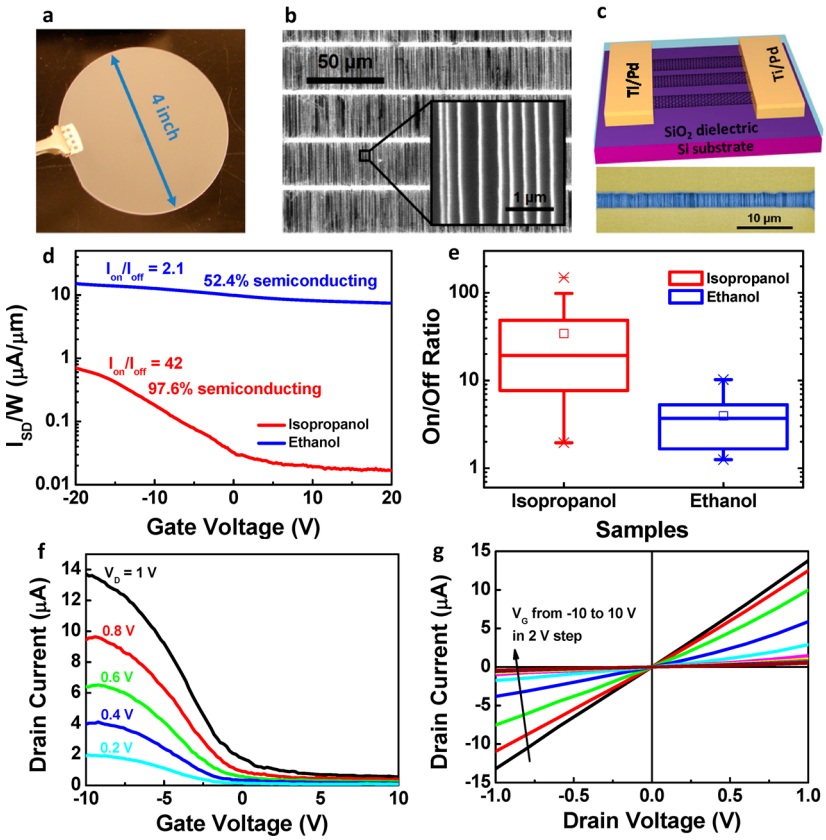

Figure 1. Wafer-scale carbon nanotube synthesis using IPA and electrical characteristics of the back-gated nanotube devices; (a) photograph of a four-inch wafer with aligned nanotubes grown; (b) SEM image of aligned nanotubes grown from IPA carbon feedstock; (c) schematic and an SEM image of a back-gated IPA-synthesized nanotube transistor; (d) $I_{SD}-V_{GS}$ curves of back-gate devices with IPA- and ethanol-synthesized nanotubes; (e) on/off ratio distribution for devices with IPA- and ethanol-synthesized carbon nanotubes; (f) transfer and (g) output characteristics of a representative back-gated transistor with IPA-grown carbon nanotubes.

devices and circuits, which would prefer highly aligned nanotubes distributed over insulating substrates. For this goal, several groups have reported the synthesis of predominantly semiconducting nanotubes on flat substrates, including approaches using ethanol/methanol mixture carbon feedstocks,[27] UV irradiation during CVD,[28] and plasma-enhanced CVD.[29−31] Nevertheless, some of those techniques require complicated processes and the introduction of UV light or plasma may decrease nanotube density. Moreover, the underlying mechanism for the selective growth of semiconducting single-walled carbon nanotubes is not well understood and some research groups have devoted efforts in this matter of hot debate.[32−35] Therefore, more research is needed to develop a simple and reliable approach for the selective synthesis of semiconducting nanotubes and to advance scientific understanding of the mechanism behind such an approach. Here, we report a facile, robust, and highly effective approach with the use of isopropyl alcohol (IPA) to synthesize predominantly semiconducting nanotubes from CVD directly. Using IPA as the feedstock, arrays of aligned semiconducting carbon nanotubes have been grown on quartz substrates up to four-inch wafers. The percentage of semiconducting nanotubes is confirmed to be 97.6% for our best sample and about 90% using both individual nanotube electrical measurements and micro-Raman spectroscopy. Furthermore, mass spectrometry was used to elucidate the underlying mechanism, which suggests that the presence of the right amount of water species from IPA decomposition played a key role for the selective growth of semiconducting single-walled nanotubes. It should be noted that we also performed nanotube synthesis on silicon substrates using our IPA-based CVD process. As an example of application, we have fabricated thin-film transistors (TFTs) from the as-grown IPA-synthesized nanotube networks on silicon substrate and an on/off ratio over 10^4 and mobility up to 116 $cm^2/(V\cdot s)$ has been achieved, which represents one of the best reported performances for TFTs up to date. The method reported here is facile and robust, and the results are highly reproducible. It could serve as a useful platform for practical and scalable carbon nanotube electronics.

RESULTS AND DISCUSSION

Figure 1 illustrates our aligned semiconducting carbon nanotube synthesis platform and the corresponding electrical performance of the as-grown nanotubes.

Aligned carbon nanotubes have been successfully synthesized on both small substrates and four-inch quartz wafers with IPA as the carbon feedstock, as shown in Figure 1a,b. A representative scanning electron microscopy (SEM) image of the nanotubes synthesized from IPA is shown in Figure 1b with an average density of 4 tubes/μm, and AFM characterization suggests a diameter distribution of 1.38 $\pm$ 0.23 nm (Figure S1 in the Supporting Information). After growth, the nanotubes were transferred from quartz growth substrates to Si/SiO_2 substrates with 500 nm SiO_2 using the method reported in our previous publication,[9] followed by the deposition of 0.5 nm Ti/50 nm Pd source/drain metal contacts. Then, the nanotubes outside the transistor channel were etched away using lithography followed by oxygen plasma. The schematic and an SEM image of a representative device consisting of horizontally aligned arrays of IPA-synthesized carbon nanotubes are shown in Figure 1c. As a comparison, we have also synthesized and studied aligned nanotubes using ethanol as the feedstock, which possess a similar nanotube density to IPA-synthesized samples (Figure S1 in the Supporting Information). Figure 1d compares the electrical characteristics of aligned nanotube transistors with IPA- (red trace) and ethanol-synthesized (blue trace) carbon nanotubes. Both devices have channel widths of 50 μm and contain approximately 200 nanotubes in the channel. The on/off ratio for the transistor using IPA-synthesized nanotubes is 42 as compared to 2.1 for the transistor using ethanol-synthesized nanotubes. If we follow the method used in a previous publication[27] and assume that the metallic nanotubes are equally conductive as the semiconducting ones in their on-state, the percentage of semiconducting nanotubes of the IPA-synthesized nanotube sample in Figure 1d is estimated to be 97.6%. As a comparison, the ethanol-synthesized nanotube sample in Figure 1d contains only roughly 52.4% of semiconducting nanotubes, which is not far away from 67% semiconducting ratio as predicted by theory and validated by experiments.[36] A number of such transistors using both IPA- and ethanol-synthesized nanotubes were measured and the on/off ratio distributions were plotted in Figure 1e. I It is obvious that the average on/off ratio of the devices using IPA-synthesized nanotubes is much higher than that using ethanol-synthesized nanotubes. The medium on/off ratios are 20 and 3.5 for IPA- and ethanol-synthesized nanotubes, respectively. On the basis of the analysis presented above, one can estimate the percentage of semiconducting nanotubes to be 95% for IPA-synthesized nanotubes and 71.4% for ethanol-synthesized nanotubes. The transfer characteristics and output characteristics for representative transistors using IPA-synthesized nanotubes are shown in Figure 1 panels f and g, respectively. Both exhibit p-type behavior and linear $I-V$ curves, indicating ohmic contacts have been achieved.

To be more rigorous, the percentage of semiconducting nanotubes is further evaluated by individual nanotube device measurements as illustrated in Figure 2. For IPA-synthesized nanotubes, we patterned narrow channel devices by using a stepper with a 0.5 μm resolution. A typical SEM image of the individual nanotube transistor is shown in Figure 2a, where the channel is defined by projection photolithography and oxygen plasma etching. A large number of such transistors were fabricated and 38 devices with one individual nanotube were selected, and their transfer characteristics were measured as shown in Figure 2b. For the measurements, the gate voltage (V_G) was swept from -20 to 20 V with a constant drain bias (V_D) of 0.2 V. From the results, we found that the percentage of devices with on/off ratios above 10 is $\sim$90%, which is much higher than the theoretical 67% semiconducting nanotubes ratio.[36] The typical transfer characteristics of metallic single nanotube transistor and semiconducting single nanotube transistor are shown in Figure 2c,d, respectively. The statistics of on/off ratios and on current of individual nanotube transistors are shown in Figure 2e,f, respectively. Furthermore, the decent on-current of such individual nanotube transistors confirms the preservation of good electrical quality in the IPA-synthesized nanotubes.

Resonant Raman spectroscopy was further used to characterize the nanotubes from different carbon feedstocks. Radial breathing modes (RBMs) were used to distinguish the semiconducting nanotubes from metallic nanotubes. A number of RBM spectra were acquired in both IPA and ethanol-synthesized nanotube samples by applying lasers with wavelengths (energy) of 533 nm (2.33 eV), 632 nm (1.98 eV), and 785 nm (1.58 eV). Figure 3 panels a and b show the Raman spectra recorded with 533 nm excitation line for IPA- (Figure 3a) and ethanol-synthesized nanotubes (Figure 3b), respectively. Raman peaks from quartz substrate are labeled with and asterisk ($*$). The figures show that all RBM frequencies distribute from 140 to 180 cm^{-1}, which belong to the semiconducting nanotubes.[37] This is as expected because the nanotubes that are in resonance with 533 nm laser excitation should be semiconducting according to the diameter distributions of as-grown nanotubes (Figure S1 in the Supporting Information). In Figure 3c,d, the RBM spectra scanned using a 632 nm laser reveal that all RBMs for IPA-synthesized nanotubes lie in the semiconducting region (Figure 3c), while RBMs for both semiconducting and metallic nanotubes were clearly observed in the ethanol-synthesized nanotubes (Figure 3d), which is consistent with our electrical measurements on both aligned nanotube arrays and individual nanotube devices. As for the 785 nm laser, no obvious RBMs were observed in both samples (data not shown), probably due to the low power of the 785 nm laser we have. With the information above, we

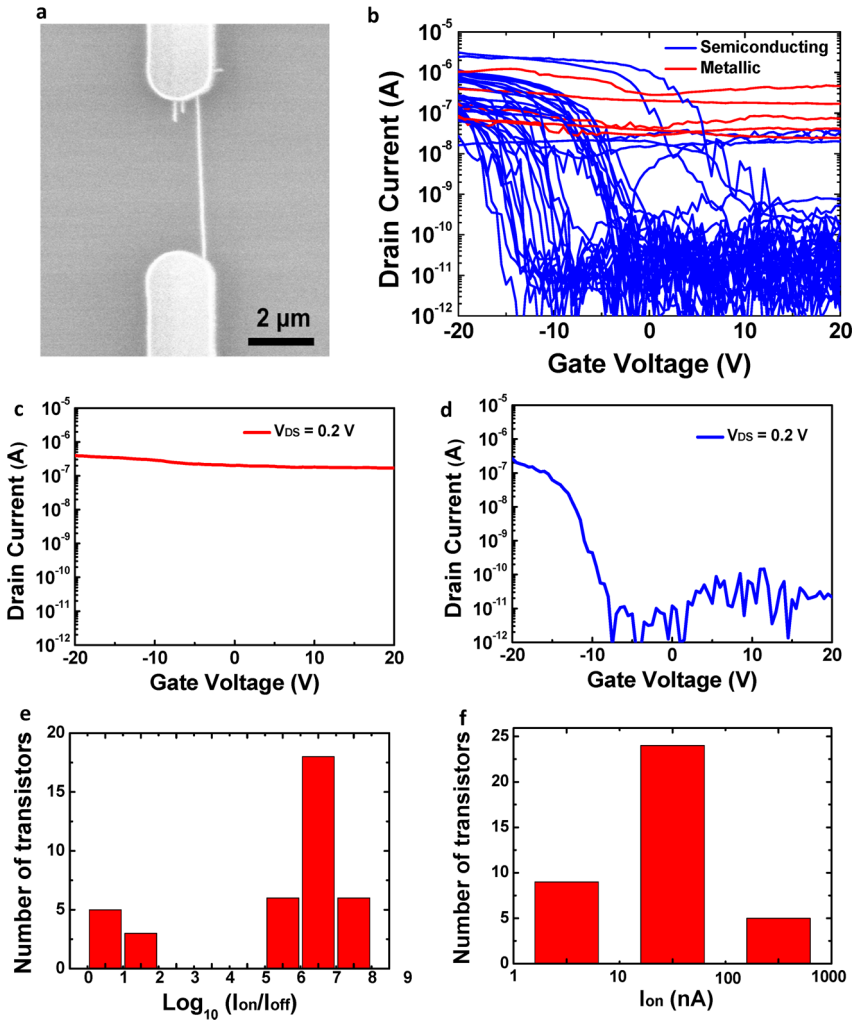

Figure 2. (a) SEM image of a representative individual nanotube device with a 4 μm channel length; (b) transfer characteristics of 38 individual nanotube transistors, with red traces representing the metallic nanotubes and blue traces representing the semiconducting ones. The percentage of devices with on/off ratio higher than 10 is around 90%. The nanotubes were grown from IPA CVD; (c) transfer characteristics of a metallic single nanotube transistor; (d) transfer characteristics of a semiconducting single nanotube transistor; (e) statistics of on/off ratio for individual nanotube devices; (f) statistics of on current for individual nanotube devices.

further conclude that nanotubes produced from IPA as carbon feedstock are predominantly semiconducting ones as compared to ethanol. To examine the quality of the as-grown nanotubes, the Raman D-band to G-band ratio at multiple locations for both samples were measured (Figure S4 in Supporting Information). The results reveal that the D/G ratios of nanotubes from IPA and ethanol are similar, ~0.04 on average, indicating overall very high quality of nanotubes synthesized using both carbon feedstocks. We note that only nanotubes in resonance with the laser energy would give Raman signal. While Raman can be a very useful tool to characterize nanotubes, Raman spectra alone does not provide definitive conclusion about what kind of nanotubes are present or not present. We have therefore carried out extensive electrical measurements on individual nanotube transistors, as discussed in Figure 2.

All the results above unambiguously confirm that predominantly semiconducting nanotubes were produced by using IPA as the carbon feedstock. While this finding is immensely useful for device applications using carbon nanotubes, it is necessary to further understand the chemical mechanism behind such selective growth behavior. We have performed a mass spectrometric[38] study to compare the CVD processes for both IPA and ethanol, and the results are shown in Figure 4. We note that mass spectrometry is a very useful tool to decipher the secret of nanotube CVD, as has been reported by Harutyunyan's group and some other groups.[39−42] In this experiment, mass spectrometry was performed with the Omnistar from Pfeiffer (model GSD301). In the measurement setup, the detector was connected to the exhaust port of a one inch tube CVD system. Using this setup, the species at the CVD exhaust port for both ethanol and IPA was quantitatively measured. Figure 4a presents the intensity *versus* mass-to-charge ratio during synthesis. To get accurate results during synthesis, both hydrogen and argon were first flowed for 5 min to purge the system of residual air.

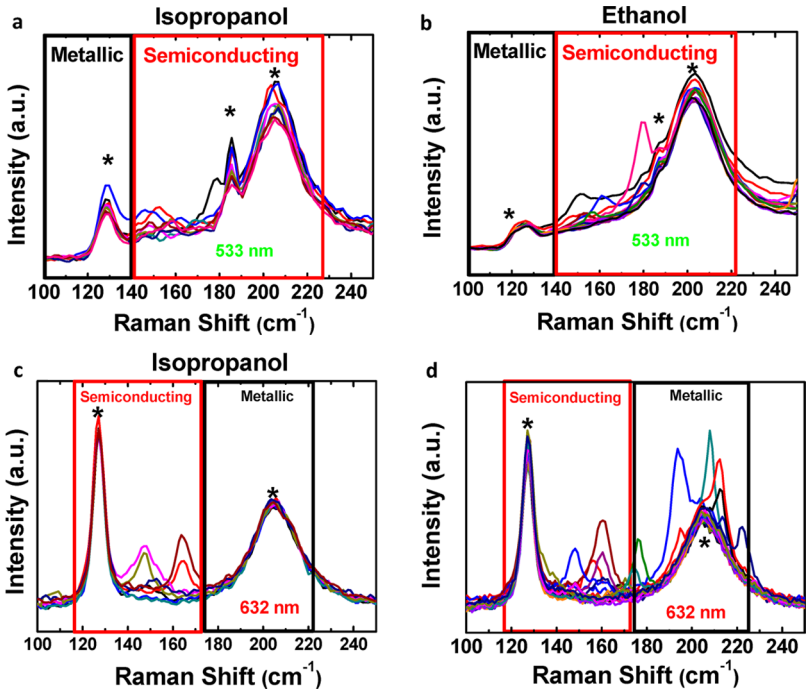

Figure 3. Micro-Raman characterization: (a) RBMs of IPA-synthesized nanotubes and (b) RBMs of ethanol-synthesized nanotubes using a 533 nm laser; (c) RBMs of IPA-synthesized nanotubes and (d) RBMs of ethanol-synthesized nanotubes using a 632 nm laser.

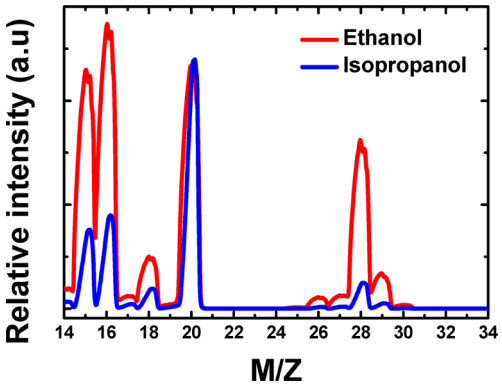

Figure 4. Mass spectra taken at the exhaust of the CVD system for ethanol (red trace) and IPA (blue trace).

After that, the temperature was increased to 900 °C with continued flow of hydrogen, and standard CVD was carried out at 900 °C by flowing argon through an ethanol or IPA bubbler. A set of mass spectra, taken with a peak at $M/Z = 20$ for Ar^{2+} (in Figure 4), was used to normalize all the curves. We took several mass spectra during the 15-min growth period (blue trace for IPA and red trace for ethanol), and the data were consistent throughout the entire synthesis period. Here, the flow rates for both synthesis processes were 300 sccm of hydrogen and 160 sccm of argon, the same as the growth procedure mentioned previously.

On the basis of the mass spectrometric results, several main species and their relative intensity are presented in Table 1. The main hydrocarbon species detected are CH_3^+, CH_4, and C_2H_4, while other species like $C_2H_2^+$ and $C_2H_5^+$ have trivial signals. By calculating the ratios between the main hydrocarbon species and water for IPA CVD, we obtained ratios of 3.9, 4.7, and 1.3 for CH_3^+, CH_4, and C_2H_4, respectively. Similarly, for ethanol CVD, we obtained ratios of 4.6, 5.4, and 3.1 for CH_3^+, CH_4, and C_2H_4, respectively. Interestingly, we noted that the hydrocarbon to water ratios are consistently lower in IPA CVD than that in ethanol CVD, indicating a relatively high concentration of the water in IPA CVD process. Particularly, we note that the ratios of C_2H_4 to H_2O are significantly different in two systems, that is, 1.3 for IPA CVD *versus* 3.1 for ethanol CVD. As water concentration has a profound effect on the selective growth of SWCNTs with a given property,[43] we believe this is the main difference between the two systems. Our results suggest that one can selectively grow predominantly semiconducting nanotubes when having the right amount of water vapor present in the CVD environment, and IPA CVD happens to provide that environment. This is consistent with a recent study

TABLE 1. Normalized Value of Relative Intensity of Possible Species from Mass Spectrometry of Synthesis Condition

M/Z	possible species	IPA	ethanol
15	CH_3^+	2.25	6.87
16	CH_4	2.7	8.15
18	H_2O	0.58	1.5
26	$C_2H_2^+$	0.049	0.32
28	C_2H_4	0.75	4.7
29	$C_2H_5^+$	0.152	1

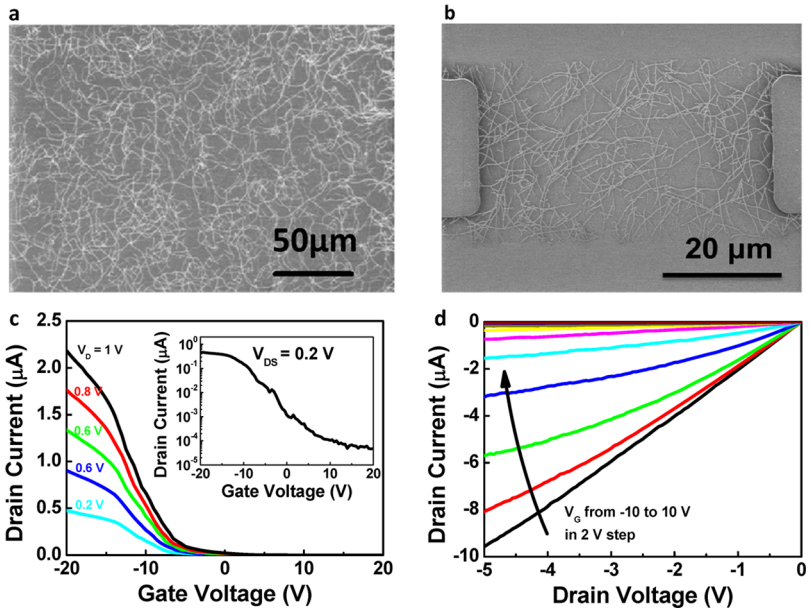

Figure 5. TFTs using networks of IPA-synthesized nanotubes: (a) SEM image of a nanotube network; (b) SEM image of a back-gated TFT; (c) transfer and (d) output characteristics of the device in panel b.

where a suitable amount of water was directly introduced into CVD process for the selective growth of semiconducting single-walled carbon nanotubes.[43] In contrast, ethanol CVD produces relatively lower water concentration than IPA CVD, and the preferential growth of semiconducting nanotubes was not observed.

The mechanism of our observed preferential growth of semiconducting nanotubes may involve multiple factors, such as suppression of metallic nanotube growth and/or selective etching of metallic nanotubes in the IPA CVD environment after their growth. To further investigate this point, we performed control experiments by loading samples predeposited with separated high purity semiconducting nanotubes (IsoNanoIntegris, 99% purity) and metallic nanotubes (IsoNanoIntegris, 98% purity) into the same IPA CVD system. The use of such separated nanotubes clearly distinguishes different behavior of semiconducting nanotubes with that of metallic ones in the IPA CVD environment. Another reason of choosing these nanotubes is that they have a very low content of metal residual, which excludes the regrowth of nanotubes from metal catalysts.[17] The separated nanotubes used in this experiment were extensively washed to remove surfactants before loading into the CVD furnace. After the samples went through the standard IPA CVD process, no noticeable change in their density and length was observed for both semiconducting and metallic nanotubes based on the comparison of the AFM images (Figure S6 in the Supporting Information). This indicates that the IPA CVD does not provide selective etching of either metallic or semiconducting nanotubes. Our results suggest that the selective growth of semiconducting nanotubes using IPA carbon feedstock mostly likely occurs through suppression of the growth of metallic nanotubes at the very beginning of nucleation. This can be understood as short caps of metallic and semiconducting nanotubes right after nucleation may have very different chemical reactivity.[28,44] We note that our post-treatment experiments using separated nanotubes cannot completely imitate the CVD process of aligned nanotube growth. As in the CVD process, the presence of metal catalysts may have influence on the growth of SWCNTs with a given property.[33] Nevertheless, our results show that the presence of the right amount of water in the IPA CVD environment leads to the preferential growth of semiconducting SWCNTs, which is consistent with some of the previous work regarding the effect of water species on SWCNT growth,[27,43] albeit with much difference in experimental details. For instance, while ethanol alone does not lead to the preferential growth of semiconducting SWCNTs, previously Ding *et al.*[27] have reported the use of mixed ethanol and methanol for preferential growth, probably because decomposition of methanol leads to more water species and OH radicals during the CVD process than ethanol alone.

The synthesis of predominantly semiconducting nanotubes using IPA may find many applications. As an example, below we report the use of IPA nanotube networks grown directly on silicon substrates for TFTs, which have great potential for display electronics, and flexible and transparent electronics.[8,45−50] While the transistors utilizing an aligned array of semiconducting nanotubes reported here exhibit on/off ratios in the range of 10 to 100, much higher on/off ratios are required for various applications and can be achieved by producing random networks of IPA-synthesized carbon nanotubes. By using such percolative carbon nanotube networks, the probability of having a metallic

nanotube conduction path between source and drain can be significantly minimized and thus high on/off ratios can be achieved as reported in our previous work using separated nanotubes.[46−50] The fabrication of the IPA-synthesized nanotube TFTs begins with the evaporation of 1 Å iron catalyst film over Si/SiO_2 substrates. The similar IPA CVD process was used to grow nanotube networks on Si/SiO_2 substrates. Source and drain electrodes (Ti/Pd) were then patterned, and back-gated transistors were fabricated after etching away the unwanted nanotubes outside the active channel region. The SEM images of the as-grown carbon nanotube thin film on a Si/SiO_2 substrate is shown in Figure 5a, and a representative nanotube TFT with a channel width of 20 μm and a channel length of 50 μm is presented in Figure 5b. As shown in the image, the nanotubes form a random network, which help to eliminate the metallic nanotube conduction path. The electrical characteristics of this device are plotted in Figure 5c,d. Figure 5c illustrates the transfer characteristics (I_D-V_G) at various drain biases in both linear and logarithm scale and Figure 5d presents the output characteristics (I_D-V_D) at various V_G biases. The on/off ratio of this transistor is up to 10^4 (Figure 5c inset), and an effective device mobility of 116 $cm^2/(V\cdot s)$ is derived, which represents one of the best mobility for thin-film transistors published up to date (Figure S7 in the Supporting Information). Our result shows the great potential of using IPA-synthesized nanotube networks for high-performance thin-film macroelectronics.

CONCLUSION

We have developed a facile, robust, and reproducible CVD approach to grow predominantly semiconducting carbon nanotubes by using IPA as the carbon feedstock. Both electrical and Raman characterization unambiguously confirms the significantly improved percentage of semiconducting nanotubes. We have also performed mass spectrometric study for different carbon feedstocks to understand the underlying mechanism behind this finding and found that water concentration may play a critical role in the observed selective growth behavior. Finally, TFTs with an on/off ratio up to 10^4 and mobility up to 116 $cm^2/(V\cdot s)$ were demonstrated using the IPA-synthesized nanotubes, which show the great potential for future applications in nanotube-based macroelectronics.

METHODS

Nanotube Synthesis. Quartz substrates were first annealed at 900 °C for 1 h in air to improve the alignment for nanotubes. To avoid wafer breakage, an extremely slow ramping rate (<1 °C/min) was used and constant gas flow rates were used during both the ramping up and growth steps as reported in our previous publication.[9] After loading the quartz or silicon substrates with deposited Fe catalyst film into growth furnace, 3600 standard cubic centimeter (sccm) of hydrogen (H_2) was used during the ramping up step. For nanotube growth, 1800 sccm of Ar flowing through an IPA bubbler (kept at 0 °C) and 3600 sccm of H_2 were used, and the growth was conducted at 900 °C . To achieve a uniform temperature throughout the entire wafer, a 9-foot-long growth furnace with a three-zone temperature controller was used for this synthesis. For the growth of nanotubes on small substrates, a one inch quartz tube furnace was used with gas flow rates of 300 sccm of H_2 and 160 sccm of Ar during the growth process, where Ar passed through a bubbler containing IPA or ethanol and was kept at 0 °C.

Conflict of Interest: The authors declare no competing financial interest.

Acknowledgment. We would like to acknowledge the collaboration of this research with King Abdulaziz City for Science and Technology (KACST), and the Focus Center Research Program (FCRP)-Center on Functional Engineered Nano Architectonics (FENA). We acknowledge financial support from Defense Threat Reduction Agency (HDTRA1-10-1-0015).

Supporting Information Available: Additional SEM and AFM images (S1), statistics of electrical properties (S2), G-band spectra of nanotubes (S3), Raman D/G ratio statistics (S4), mass spectrometry (S5), AFM images of semiconducting and metallic nanotubes before and after IPA CVD process (S6), effective device mobility (S7), radial breathing modes spectra of nanotubes (S8). This material is available free of charge *via* the Internet at http://pubs.acs.org.

REFERENCES AND NOTES

1. Tans, S. J.; Devoret, M. H.; Dai, H. J.; Thess, A.; Smalley, R. E.; Geerligs, L. J.; Dekker, C. Individual Single-Wall Carbon Nanotubes as Quantum Wires. *Nature* **1997**, *386*, 474–477.
2. Dresselhaus, M. S.; Dresselhaus, G.; Avouris, P. *Carbon Nanotubes: Synthesis, Structure, Properties, and Applications;* Springer: New York, 2001.
3. Bockrath, M.; Cobden, D. H.; McEuen, P. L.; Chopra, N. G.; Zettl, A.; Thess, A.; Smalley, R. E. Single-Electron Transport in Ropes of Carbon Nanotubes. *Science* **1997**, *275*, 1922–1925.
4. Tans, S. J.; Verschueren, A. R. M.; Dekker, C. Room-Temperature Transistor Based on a Single Carbon Nanotube. *Nature* **1998**, *393*, 49–52.
5. Javey, A.; Guo, J.; Wang, Q.; Lundstrom, M.; Dai, H. J. Ballistic Carbon Nanotube Field-Effect Transistors. *Nature* **2003**, *424*, 654–657.
6. Chen, Z. H.; Appenzeller, J.; Lin, Y. M.; Sippel-Oakley, J.; Rinzler, A. G.; Tang, J. Y.; Wind, S. J.; Solomon, P. M.; Avouris, P. An Integrated Logic Circuit Assembled on a Single Carbon Nanotube. *Science* **2006**, *311*, 1735–1735.
7. Kang, S. J.; Kocabas, C.; Ozel, T.; Shim, M.; Pimparkar, N.; Alam, M. A.; Rotkin, S. V.; Rogers, J. A. High-Performance Electronics Using Dense, Perfectly Aligned Arrays of Single-Walled Carbon Nanotubes. *Nat. Nanotechnol.* **2007**, *2*, 230–236.
8. Sun, D. M.; Timmermans, M. Y.; Tian, Y.; Nasibulin, A. G.; Kauppinen, E. I.; Kishimoto, S.; Mizutani, T.; Ohno, Y. Flexible High-Performance Carbon Nanotube Integrated Circuits. *Nat. Nanotechnol.* **2011**, *6*, 156–161.
9. Ryu, K.; Badmaev, A.; Wang, C.; Lin, A.; Patil, N.; Gomez, L.; Kumar, A.; Mitra, S.; Wong, H. S. P.; Zhou, C. W. Cmos-Analogous Wafer-Scale Nanotube-on-Insulator Approach for Submicrometer Devices and Integrated Circuits Using Aligned Nanotubes. *Nano Lett.* **2009**, *9*, 189–197.
10. Ismach, A.; Segev, L.; Wachtel, E.; Joselevich, E. Atomic-Step-Templated Formation of Single Wall Carbon Nanotube Patterns. *Angew. Chem., Int. Ed.* **2004**, *43*, 6140–6143.
11. Han, S.; Liu, X. L.; Zhou, C. W. Template-Free Directional Growth of Single-Walled Carbon Nanotubes on a- and r-Plane Sapphire. *J. Am. Chem. Soc.* **2005**, *127*, 5294–5295.
12. Kocabas, C.; Hur, S. H.; Gaur, A.; Meitl, M. A.; Shim, M.; Rogers, J. A. Guided Growth of Large-Scale, Horizontally

Aligned Arrays of Single-Walled Carbon Nanotubes and Their Use in Thin-Film Transistors. *Small* **2005**, *1*, 1110–1116.
13. Liu, X. L.; Ryu, K.; Badmaev, A.; Han, S.; Zhou, C. W. Diameter Dependence of Aligned Growth of Carbon Nanotubes on a-Plane Sapphire Substrates. *J. Phys. Chem. C.* **2008**, *112*, 15929–15933.
14. Kocabas, C.; Dunham, S.; Cao, Q.; Cimino, K.; Ho, X. N.; Kim, H. S.; Dawson, D.; Payne, J.; Stuenkel, M.; Zhang, H.; *et al*. High-Frequency Performance of Submicrometer Transistors That Use Aligned Arrays of Single-Walled Carbon Nanotubes. *Nano Lett.* **2009**, *9*, 1937–1943.
15. Wang, C. A.; Ryu, K. M.; De Arco, L. G.; Badmaev, A.; Zhang, J. L.; Lin, X.; Che, Y. C.; Zhou, C. W. Synthesis and Device Applications of High-Density Aligned Carbon Nanotubes Using Low-Pressure Chemical Vapor Deposition and Stacked Multiple Transfer. *Nano Res.* **2010**, *3*, 831–842.
16. Hong, S. W.; Banks, T.; Rogers, J. A. Improved Density in Aligned Arrays of Single-Walled Carbon Nanotubes by Sequential Chemical Vapor Deposition on Quartz. *Adv. Mater.* **2010**, *22*, Cp30–Cp30.
17. Zhou, W. W.; Ding, L.; Yang, S.; Liu, J. Synthesis of High-Density, Large-Diameter, and Aligned Single-Walled Carbon Nanotubes by Multiple-Cycle Growth Methods. *ACS Nano* **2011**, *5*, 3849–3857.
18. Collins, P. C.; Arnold, M. S.; Avouris, P. Engineering Carbon Nanotubes and Nanotube Circuits Using Electrical Breakdown. *Science* **2001**, *292*, 706–709.
19. Krupke, R.; Hennrich, F.; von Lohneysen, H.; Kappes, M. M. Separation of Metallic from Semiconducting Single-Walled Carbon Nanotubes. *Science* **2003**, *301*, 344–347.
20. Arnold, M. S.; Green, A. A.; Hulvat, J. F.; Stupp, S. I.; Hersam, M. C. Sorting Carbon Nanotubes by Electronic Structure Using Density Differentiation. *Nat. Nanotechnol.* **2006**, *1*, 60–65.
21. Tanaka, T.; Jin, H.; Miyata, Y.; Fujii, S.; Suga, H.; Naitoh, Y.; Minari, T.; Miyadera, T.; Tsukagoshi, K.; Kataura, H. Simple and Scalable Gel-Based Separation of Metallic and Semiconducting Carbon Nanotubes. *Nano Lett.* **2009**, *9*, 1497–1500.
22. Tu, X. M.; Manohar, S.; Jagota, A.; Zheng, M. DNA Sequence Motifs for Structure-Specific Recognition and Separation of Carbon Nanotubes. *Nature* **2009**, *460*, 250–253.
23. Yu, B.; Liu, C.; Hou, P. X.; Tian, Y.; Li, S. S.; Liu, B. L.; Li, F.; Kauppinen, E. I.; Cheng, H. M. Bulk Synthesis of Large Diameter Semiconducting Single-Walled Carbon Nanotubes by Oxygen-Assisted Floating Catalyst Chemical Vapor Deposition. *J. Am. Chem. Soc.* **2011**, *133*, 5232–5235.
24. Bachilo, S. M.; Balzano, L.; Herrera, J. E.; Pompeo, F.; Resasco, D. E.; Weisman, R. B. Narrow (*N*,*M*)-Distribution of Single-Walled Carbon Nanotubes Grown Using a Solid Supported Catalyst. *J. Am. Chem. Soc.* **2003**, *125*, 11186–11187.
25. Jorio, A.; Santos, A. P.; Ribeiro, H. B.; Fantini, C.; Souza, M.; Vieira, J. P. M.; Furtado, C. A.; Jiang, J.; Saito, R.; Balzano, L., *et al*. Quantifying Carbon-Nanotube Species with Resonance Raman Scattering. *Phys. Rev. B.* **2005**, *72*.
26. He, M. S.; Liu, B. L.; Chernov, A. I.; Obraztsova, E. D.; Kauppi, I.; Jiang, H.; Anoshkin, I.; Cavalca, F.; Hansen, T. W.; Wagner, J. B.; *et al*. Growth Mechanism of Single-Walled Carbon Nanotubes on Iron-Copper Catalyst and Chirality Studies by Electron Diffraction. *Chem. Mater.* **2012**, *24*, 1796–1801.
27. Ding, L.; Tselev, A.; Wang, J. Y.; Yuan, D. N.; Chu, H. B.; McNicholas, T. P.; Li, Y.; Liu, J. Selective Growth of Well-Aligned Semiconducting Single-Walled Carbon Nanotubes. *Nano Lett.* **2009**, *9*, 800–805.
28. Hong, G.; Zhang, B.; Peng, B. H.; Zhang, J.; Choi, W. M.; Choi, J. Y.; Kim, J. M.; Liu, Z. F. Direct Growth of Semiconducting Single-Walled Carbon Nanotube Array. *J. Am. Chem. Soc.* **2009**, *131*, 14642–+.
29. Li, Y. M.; Mann, D.; Rolandi, M.; Kim, W.; Ural, A.; Hung, S.; Javey, A.; Cao, J.; Wang, D. W.; Yenilmez, E.; *et al*. Preferential Growth of Semiconducting Single-Walled Carbon Nanotubes by a Plasma Enhanced CVD Method. *Nano Lett.* **2004**, *4*, 317–321.
30. Qu, L. T.; Du, F.; Dai, L. M. Preferential Syntheses of Semiconducting Vertically Aligned Single-Walled Carbon Nanotubes for Direct Use in FETS. *Nano Lett.* **2008**, *8*, 2682–2687.
31. Ghorannevis, Z.; Kato, T.; Kaneko, T.; Hatakeyama, R. Narrow-Chirality Distributed Single-Walled Carbon Nanotube Growth from Nonmagnetic Catalyst. *J. Am. Chem. Soc.* **2010**, *132*, 9570–9572.
32. Chiang, W. H.; Sankaran, R. M. Linking Catalyst Composition to Chirality Distributions of as-Grown Single-Walled Carbon Nanotubes by Tuning Ni_xFe_{1-x} Nanoparticles. *Nat. Mater.* **2009**, *8*, 882–886.
33. Harutyunyan, A. R.; Chen, G. G.; Paronyan, T. M.; Pigos, E. M.; Kuznetsov, O. A.; Hewaparakrama, K.; Kim, S. M.; Zakharov, D.; Stach, E. A.; Sumanasekera, G. U. Preferential Growth of Single-Walled Carbon Nanotubes with Metallic Conductivity. *Science* **2009**, *326*, 116–120.
34. Koziol, K. K. K.; Ducati, C.; Windle, A. H. Carbon Nanotubes with Catalyst Controlled Chiral Angle. *Chem. Mater.* **2010**, *22*, 4904–4911.
35. Reich, S.; Li, L.; Robertson, J. Control the Chirality of Carbon Nanotubes by Epitaxial Growth. *Chem. Phys. Lett.* **2006**, *421*, 469–472.
36. Kim, W.; Choi, H. C.; Shim, M.; Li, Y. M.; Wang, D. W.; Dai, H. J. Synthesis of Ultralong and High Percentage of Semiconducting Single-Walled Carbon Nanotubes. *Nano Lett.* **2002**, *2*, 703–708.
37. Dresselhaus, M. S.; Dresselhaus, G.; Saito, R.; Jorio, A. Raman Spectroscopy of Carbon Nanotubes. *Phys. Rep.* **2005**, *409*, 47–99.
38. Gross, J. H. *Mass Spectrometry: A Textbook*; Springer: New York, 2004.
39. Xu., Y.-Q.; Flor., E.; Schmidt., H.; Smalley., R. E.; Hauge, R. H. Effects of Atomic Hydrogen and Active Carbon Species in 1mm Vertically Aligned Single-Walled Carbon Nanotube Growth. *Appl. Phys. Lett.* **2006**, *89*, 123116–123118.
40. Mora., E.; Pigos., J. M.; Ding., F.; Yakobson., B. I.; Harutyunyan., A. R. Low-Temperature Single-Wall Carbon Nanotubes Synthesis: Feedstock Decomposition Limited Growth. *J. Am. Chem. Soc.* **2008**, *130*, 11840–11841.
41. Mora, E.; Harutyunyan, A. R. Study of Single-Walled Carbon Nanotubes Growth *via* the Catalyst Lifetime. *J. Phys. Chem. C* **2008**, *112*, 4805–4812.
42. Harutyunyan, A. R.; Kuznetsov, O. A.; Brooks, C. J.; Mora, E.; Chen, G. G. Thermodynamics Behind Carbon Nanotube Growth *via* Endothermic Catalytic Decomposition Reaction. *ACS Nano* **2009**, *3*, 379–385.
43. Li, P.; Zhang, J. Sorting out Semiconducting Single-Walled Carbon Nanotube Arrays by Preferential Destruction of Metallic Tubes Using Water. *J. Mater. Chem.* **2011**, *21*, 11815–11821.
44. Joselevich, E. Electronic Structure and Chemical Reactivity of Carbon Nanotubes: A Chemist's View. *Chemphyschem.* **2004**, *5*, 619–624.
45. Engel, M.; Small, J. P.; Steiner, M.; Freitag, M.; Green, A. A.; Hersam, M. C.; Avouris, P. Thin Film Nanotube Transistors Based on Self-Assembled, Aligned, Semiconducting Carbon Nanotube Arrays. *ACS Nano* **2008**, *2*, 2445–2452.
46. Wang, C.; Zhang, J. L.; Ryu, K. M.; Badmaev, A.; De Arco, L. G.; Zhou, C. W. Wafer-Scale Fabrication of Separated Carbon Nanotube Thin-Film Transistors for Display Applications. *Nano Lett.* **2009**, *9*, 4285–4291.
47. Wang, C. A.; Zhang, J. L.; Zhou, C. W. Macroelectronic Integrated Circuits Using High-Performance Separated Carbon Nanotube Thin-Film Transistors. *ACS Nano* **2010**, *4*, 7123–7132.
48. Zhang, J. L.; Wang, C.; Fu, Y.; Che, Y. C.; Zhou, C. W. Air-Stable Conversion of Separated Carbon Nanotube Thin-Film Transistors from P-Type to N-Type Using Atomic Layer Deposition of High-Kappa Oxide and Its Application in CMOS Logic Circuits. *ACS Nano* **2011**, *5*, 3284–3292.
49. Zhang, J. L.; Fu, Y.; Wang, C.; Chen, P. C.; Liu, Z. W.; Wei, W.; Wu, C.; Thompson, M. E.; Zhou, C. W. Separated Carbon

Nanotube Macroelectronics for Active Matrix Organic Light-Emitting Diode Displays. *Nano Lett.* **2011**, *11*, 4852–4858.
50. Chen, P. C.; Fu, Y.; Aminirad, R.; Wang, C.; Zhang, J. L.; Wang, K.; Galatsis, K.; Zhou, C. W. Fully Printed Separated Carbon Nanotube Thin Film Transistor Circuits and Its Application in Organic Light Emitting Diode Control. *Nano Lett.* **2011**, *11*, 5301–5308.